SUPPLEMENTARY FIGURES

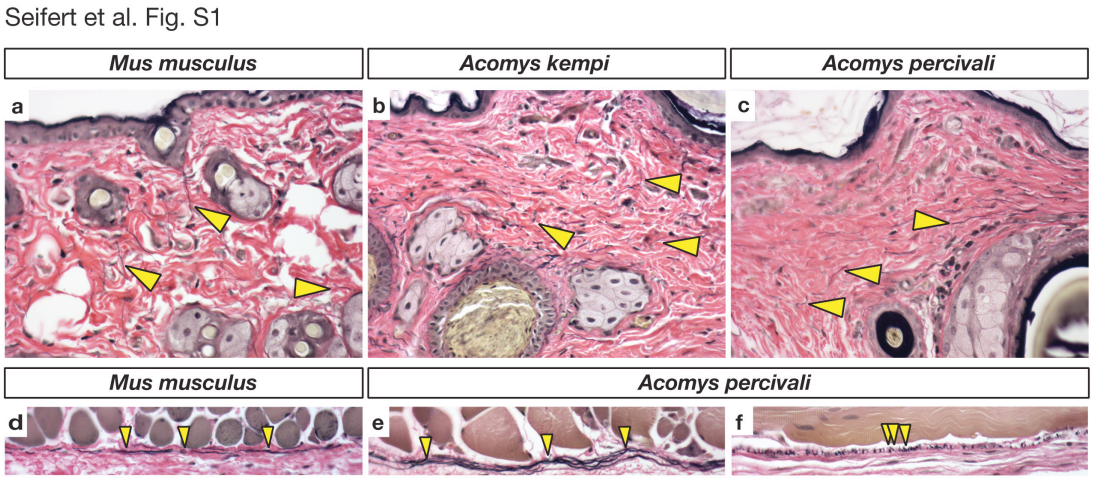

Figure S1 | Elastin fibers are distributed similarly throughout the skin of *Acomys* and *Mus*. **(a-c)** We stained full thickness skin for the presence of elastin fibers and found that elastin was distributed throughout the dermis in *M. musculus* (**a**) *A. wilsoni* (**b**) and *A. percivali* (**c**) in a similar pattern (yellow arrows). In all three species elastin fibers were more prominent near hair follicles and sebaceous glands. (**d-f**) Elastin fibers formed a meshwork underneath the panniculus carnosus that was similar across species. Fibers were orientated perpendicular to the cranial/caudal axis such that associated fibers were visible in transverse section (d-e) and longitudinally were visible as individual fibers in cross-section.

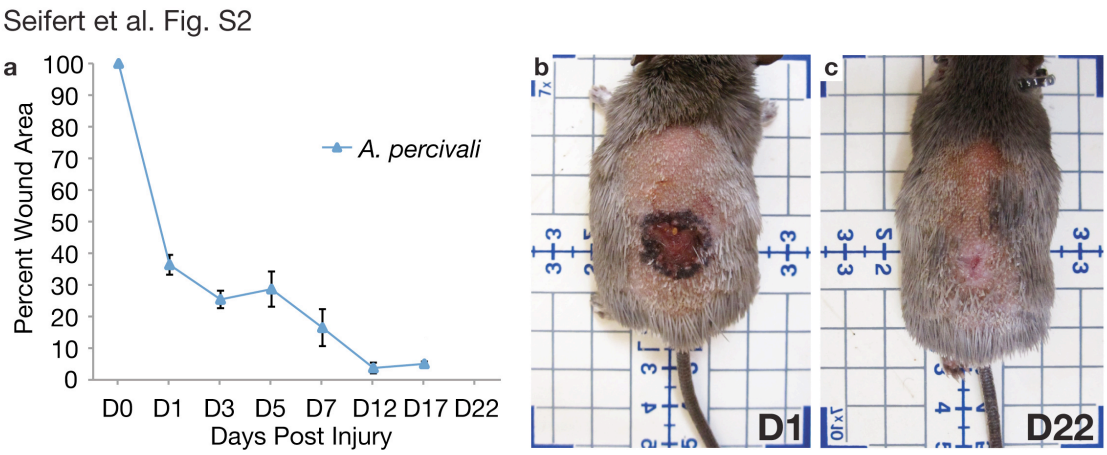

Figure S2 | Large 1.5cm full thickness excisional (FTE) wounds heal primarily through contraction. (a) 1.5cm circular FTE wounds are reduced to ~5% of the original wound area 12 days post injury in *A. percivali*. (**b-c**) Position of large FTE wounds in *A. percivali* during the healing process showing the degree of contraction and the resulting wound bed. Error bars in (a) represent s.e.m., n=12.

Seifert et al. Fig. S3

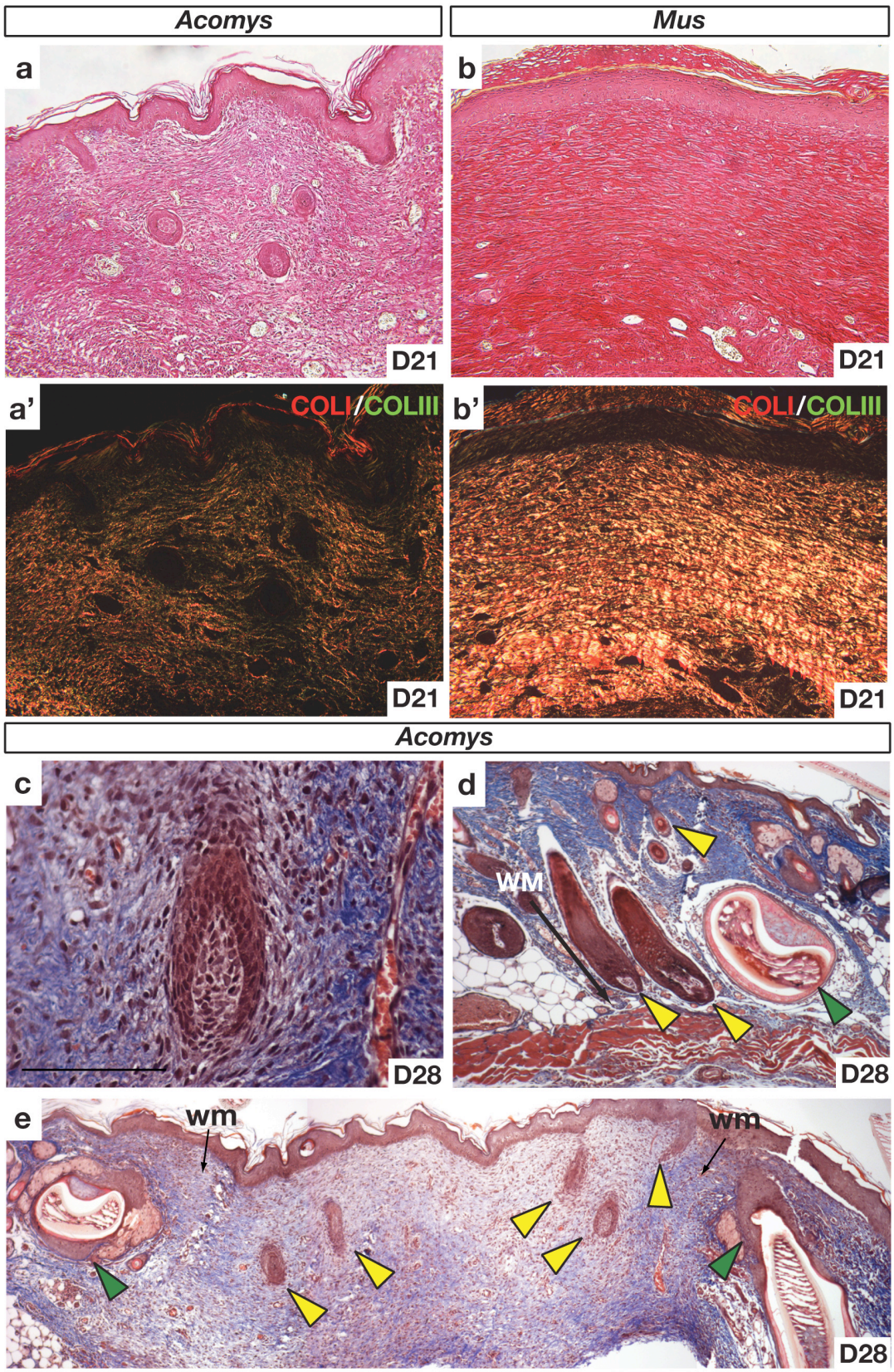

Figure S3 | Differences in collagen composition of extracellular matrix (ECM) during follicle regeneration in *Acomys* and scarring in *Mus*. (a-b') Picrosirius red staining of the wound bed at D21 post injury in *Acomys* and *Mus*. **(a-a')** *Acomys* ECM has a basketweave[1] orientation typical of unwounded dermis and shows abundant collagen type III throughout the extracellular matrix. The relative abundance of collagen type III in the wound bed resembles the fetal composition of dermis where collagen type III is in greater abundance[2,3]. **(b'b')** The new ECM in *Mus* is dominated by collagen type I and is oriented in a dense parallel network of fibers underlying the epidermis. No new follicles are present in the wound bed of *Mus* at D21. (**c**) New follicle developing in the wound bed in association with dermal papilla. (**d-e**) New follicles forming in the wound bed (yellow arrows) can be differentiated from the mature form of old follicles (green arrows) that have grown into the wound bed from outside the wound margin (WM).

Figure S4 | Regenerating hair follicles progress through normal stages of hair follicle development and exhibit similar patterns of epidermal proliferation. (a-c) Ki67 staining of proliferating epidermal cells in regenerating hair follicles in the ear at (a) hair placode stage, (b) hair peg stage and (c) showing formation of dermal papilla. These stages are typical of developing hair follicles[4]. Scale bars = 100µm.

Seifert et al. Fig. S5

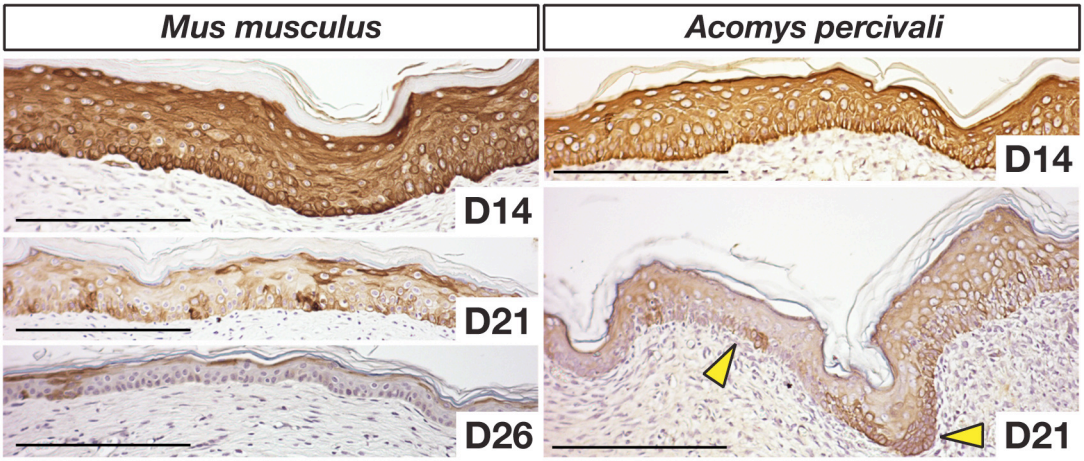

Figure S5 | Keratin-17 is present in the neoepidermis of *Mus* and *Acomys,* but disappears in *Mus* while localizing to regenerating hair follicles in *Acomys*. Keratin-17 (KRT17) staining in the neoepidermis overlying the wound bed. In *Mus*, KRT17 is present 14 days post injury throughout the epidermis . At D21, KRT17 is present in a few scattered keratinocytes that lack any recognizable structure and by D28 is absent from the epidermis. In contrast, at D21 in *Acomys*, KRT17, which was also expressed throughout the epidermis at D14, becomes restricted to developing hair placodes and follicles (yellow arrows). Scale bars = 100µm.

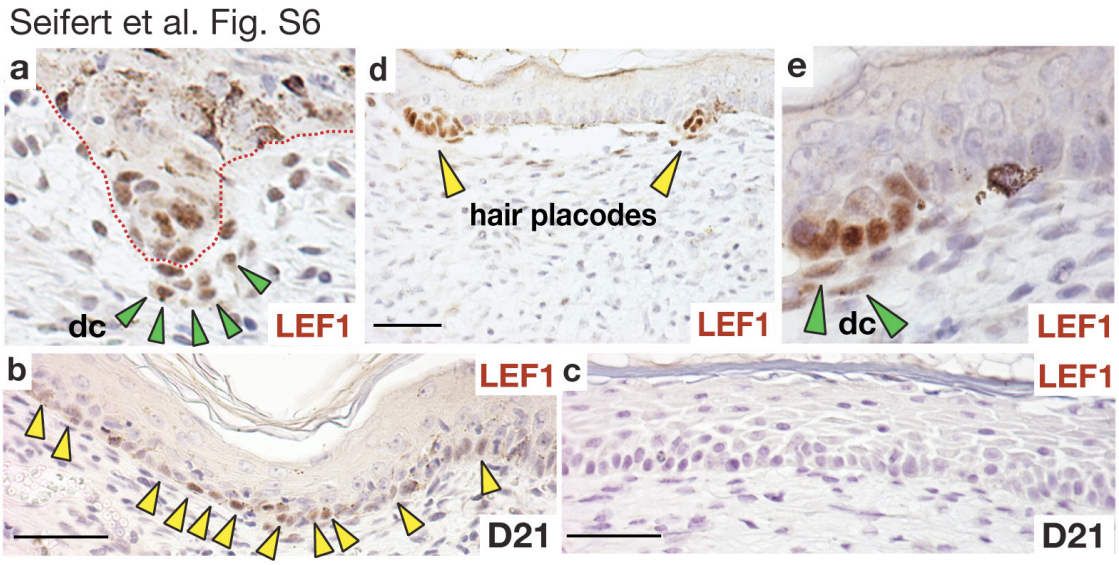

Figure S6 | Wnt-signaling pathway is active in regenerating hair follicles in the skin and ear. (a) LEF1 protein is present in the nucleus of condensing dermal cells (dc; green arrows) beneath the hair germ and in some epidermal cells of the hair germ. **(b-c)** Nuclear LEF1 protein is present in some basal keratinocytes in the epidermis prior to placode formation in *Acomys* (b) whereas LEF1 is not present in the epidermis of *Mus* (c). Yellow arrows show cytoplasmic localization in the hair peg. **(d-e)** LEF1 also localizes to regenerating hair follicles in the ear. Scale bars = 100µm.

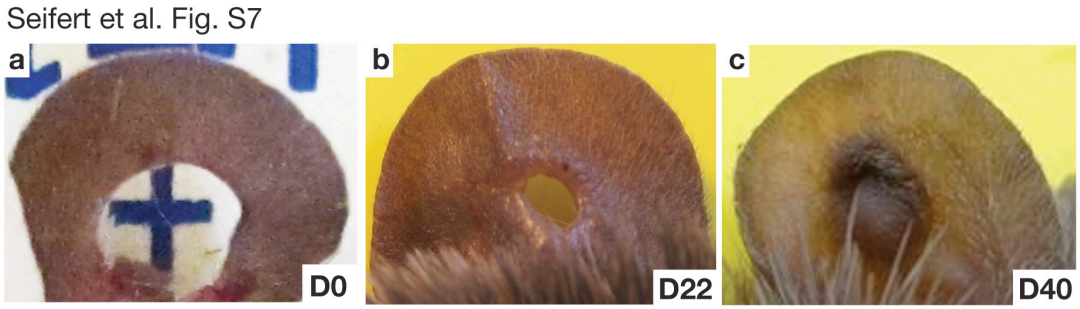

Figure S7 | *A. kempi* regenerate 4mm punches through the ear pinna. **(a-c)** Representative time series of ear hole regeneration in *A. kempi*. Examples of regenerating ear punch in dorsal (a, b) and ventral views (c). There was variation in the speed of closure, ranging from 20 to 50 days among individuals.

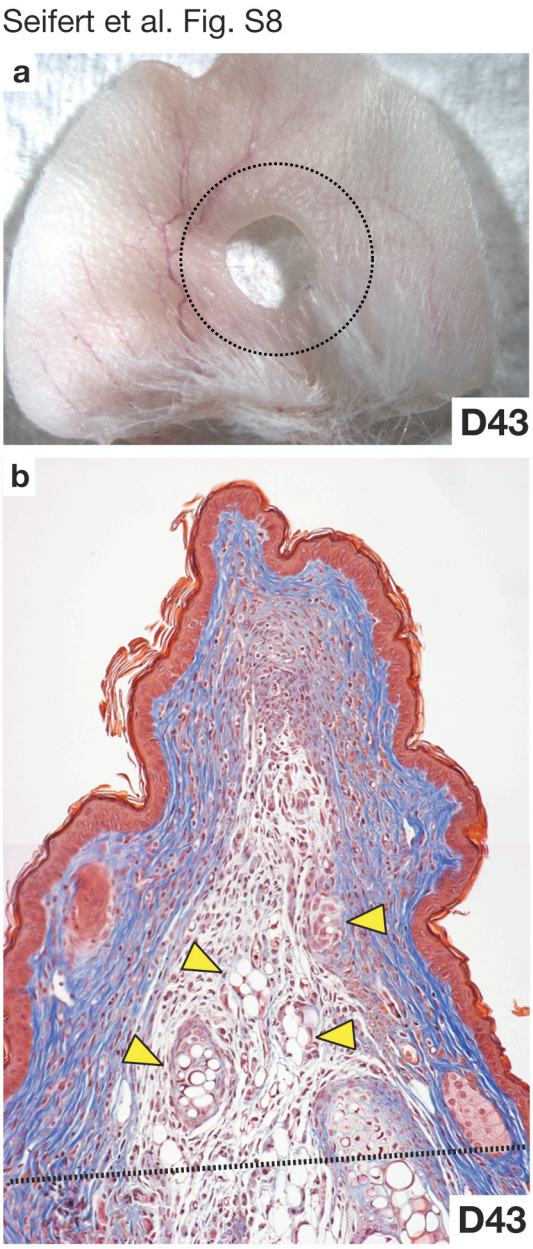

Figure S8 | *Mus* cannot regenerate 4mm ear punches but new cartilage condensations are present distal to the amputation plane. (a) Hyperplastic growth allows for limited closure of 4mm ear punches in *Mus*. Black circle represents original ear punch. **(b)** A section through partially healed ear punch shows new cartilage

condensations (yellow arrows) distal to the original injury (black dotted line). No regenerated hair follicles are present.

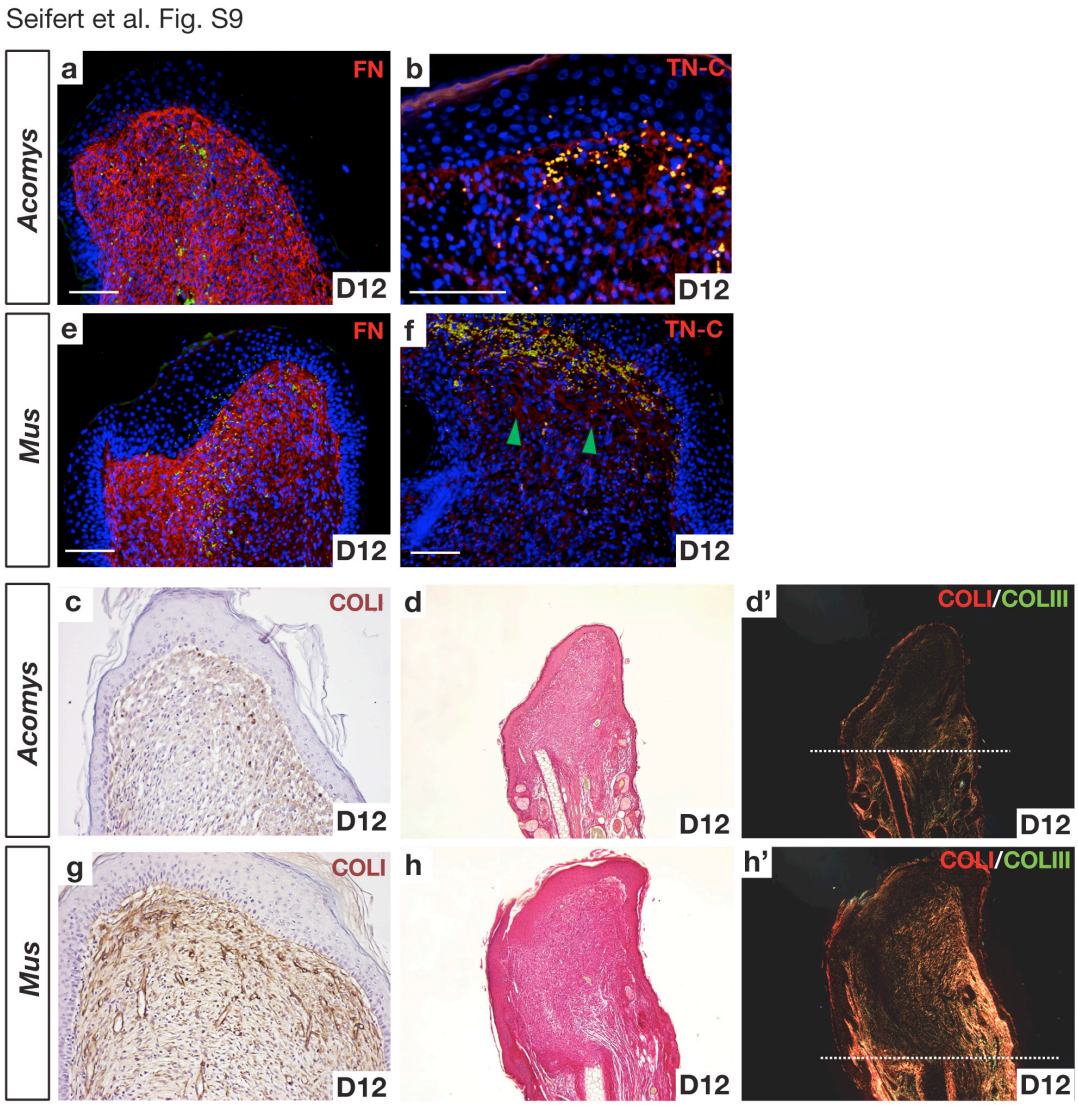

Figure S9 | Early ECM composition during regeneration in *Acomys* and repair in *Mus*. Immunostaining for FN **(a, e)**, TN-C **(b, f)**, and collagen type I **(c, g)**. FN is highly expressed throughout blastemal cells in both *Acomys* and *Mus*. **(b, f)** TN-C is present at lower levels compared to FN throughout the blastema in both animals (green arrows). **(c, g)** Collagen type I is present at higher levels in *Mus* compared to *Acomys*.

(d-d', h-h') Picrosirius red staining shows relative proportions of collagen type I (red/orange) and collagen type III (green). (d-d') Total collagen is present at very low levels distal to the amputation plane (white dotted line) in *Acomys*. Some collagen type III (green) is present, but very little collagen type I (red/orange) is visible. (h-h') In contrast to *Acomys*, total collagen is much more abundant in *Mus* with collagen type I more prominent compared to collagen type III.

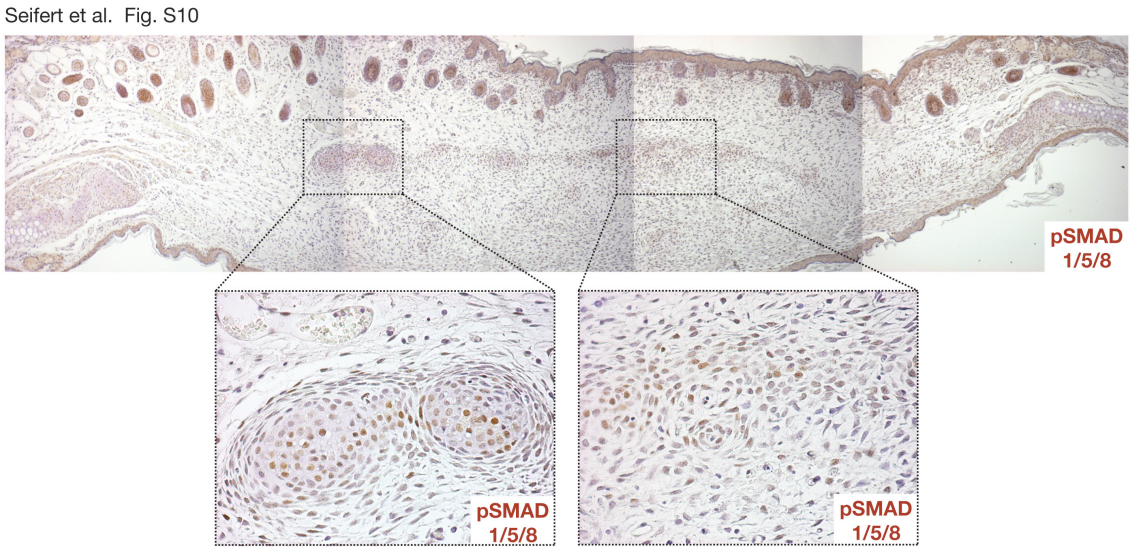

Figure S10 | Bmp-signaling is upregulated during chondrocyte condensation. Phosphorylated SMAD 1/5/8 is a readout of canonical Bmp-signaling and is present in regenerated cartilage cells and condensing chondrocytes.

SUPPLEMENTARY REFERENCES

1 Ferguson, M. W. & O'Kane, S. Scar-free healing: from embryonic mechanisms to adult therapeutic intervention. *Philos Trans R Soc Lond B Biol Sci* **359**, 839-850, doi:10.1098/rstb.2004.1475 LQD5XA1X2TJ3L73X [pii] (2004).

2 Adzick, N. S. *Fetal wound healing*. (Elsevier, 1992).

[3] Merkel, J. R., Dipaolo, B. R., Hallock, G. G. & Rice, D. C. Type-I and Type-Iii Collagen Content of Healing Wounds in Fetal and Adult-Rats. *Proceedings of the Society for Experimental Biology and Medicine* **187**, 493-497 (1988).

[4] Schmidt-Ullrich, R. & Paus, R. Molecular principles of hair follicle induction and morphogenesis. *Bioessays* **27**, 247-261, doi:10.1002/bies.20184 (2005).